Supplementary Information

Catalytic Effects of Iron Adatoms in Poly(*para*-phenylene) Synthesis on Rutile TiO_2(110)

Mohammadreza Rostami[1], Biao Yang[1,2,*], Xiaochuan Ma[3], Sifan You[2], Jin Zhou[3], Meng Zhang[2], Xuefeng Cui[3], Haiming Zhang[2], Francesco Allegretti[1], Bing Wang[3], Lifeng Chi[2,*], Johannes V. Barth[1,*]

[1] Physics Department E20, School of Natural Sciences, Technical University of Munich, Garching, 85748, Germany

[2] Institute of Functional Nano & Soft Materials (FUNSOM), Joint International Research Laboratory of Carbon-Based Functional Materials and Devices, Soochow University, Suzhou, 215123, P. R. China

[3] Hefei National Research Center for Physical Sciences at the Microscale and Synergetic Innovation Center of Quantum Information & Quantum Physics, New Cornerstone Science Laboratory, University of Science and Technology of China, Hefei, 230026, China

* Email: jvb@tum.de; chilf@suda.edu.cn; yangbiao@suda.edu.cn

SUPPLEMENT MEASUREMENTS AND RESULTS

In Fig. S1g, STS exhibits a band gap of about 3.3 eV for rutile TiO_2 (110) surface [1-5].

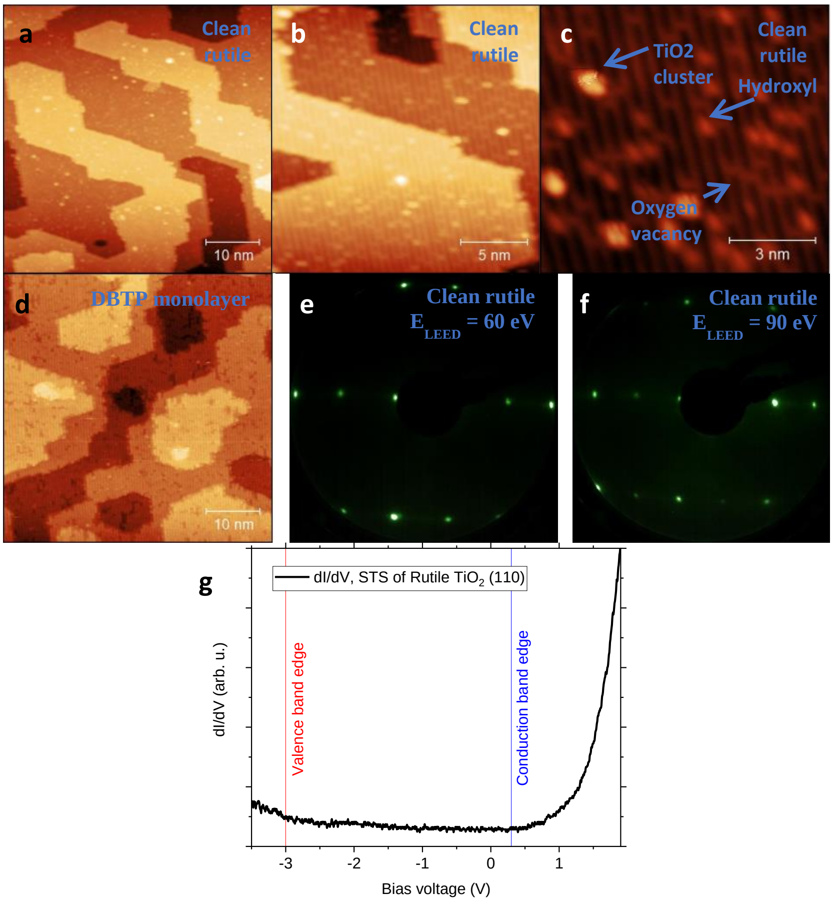

Fig. S1. STM images of a clean rutile TiO_2 (110) surface; (a) The distance between the brightest and darkest points (Z-height) = 1.32 nm, V_s = -1 V, I_t = 10 pA. (b) Z-height = 0.80 nm, V_s = -1 V, I_t = 10 pA. (c) Z-height = 0.25 nm, V_s = -1 V, I_t = 10 pA. (d) An STM image of a DBTP monolayer after deposition at room temperature on a rutile TiO_2 surface; Z-height = 1.44 nm, V_s = -1 V, I_t = 10 pA. STM acquisition temperature: 77 K. (1×1) LEED patterns of a clean rutile TiO_2 (110) surface with (e)

E_{LEED} = 60 eV and (f) E_{LEED} = 90 eV. (g) Tunneling spectra of rutile TiO_2 (110). STM / STS data acquisition at T=77 K.

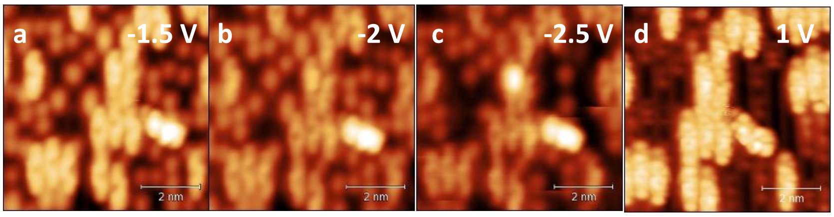

Fig. S2. Bias-dependent STM images of DBTP dimers after annealing at 400 K on a rutile TiO_2(110) surface and subsequent coupling. (a) Z-height = 0.22 nm, V_s = -1.5 V, I_t = 10 pA. (b) Z-height = 0.22 nm, V_s = -2 V, I_t = 10 pA. (c) Z-height = 0.22 nm, V_s = -2.5 V, I_t = 10 pA. (d) Z-height = 0.22 nm, V_s = 1 V, I_t = 10 pA. STM acquisition temperature: 77 K.

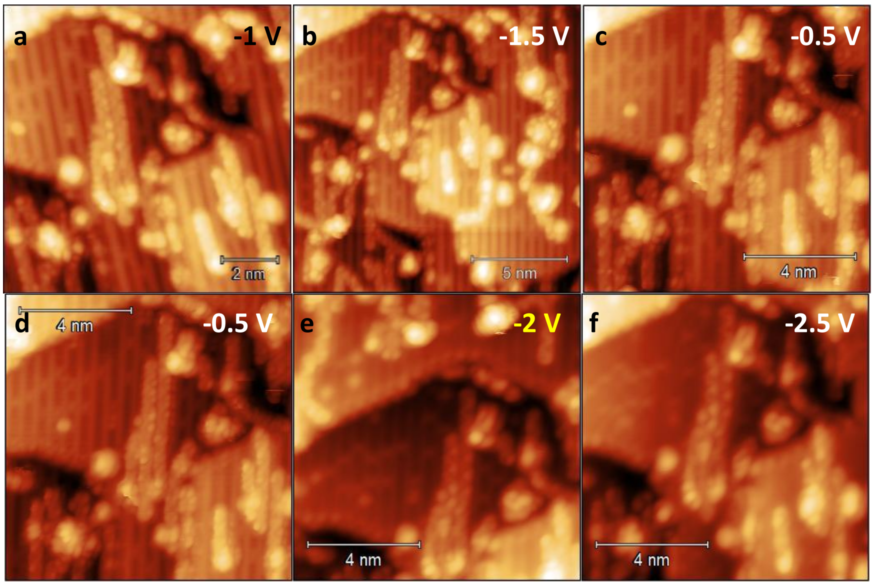

Fig. S3. Bias-dependent STM images of 3AGNRs after annealing at 600 K on a rutile TiO_2 (110) surface. (a) Z-height = 0.56 nm, V_s = -1 V, I_t = 10 pA. (b) Z-height = 0.65 nm, V_s = -1.5 V, I_t = 10 pA. (c) Z-height = 0.64 nm, V_s = -0.5 V, I_t = 10 pA. (d) Z-height = 0.71 nm, V_s = -0.5 V, I_t = 10 pA. (e) Z-height = 0.66 nm, V_s = -2 V, I_t = 10 pA. (f) Z-height = 0.61 nm, V_s = -2.5 V, I_t = 10 pA. STM acquisition temperature: 77 K.

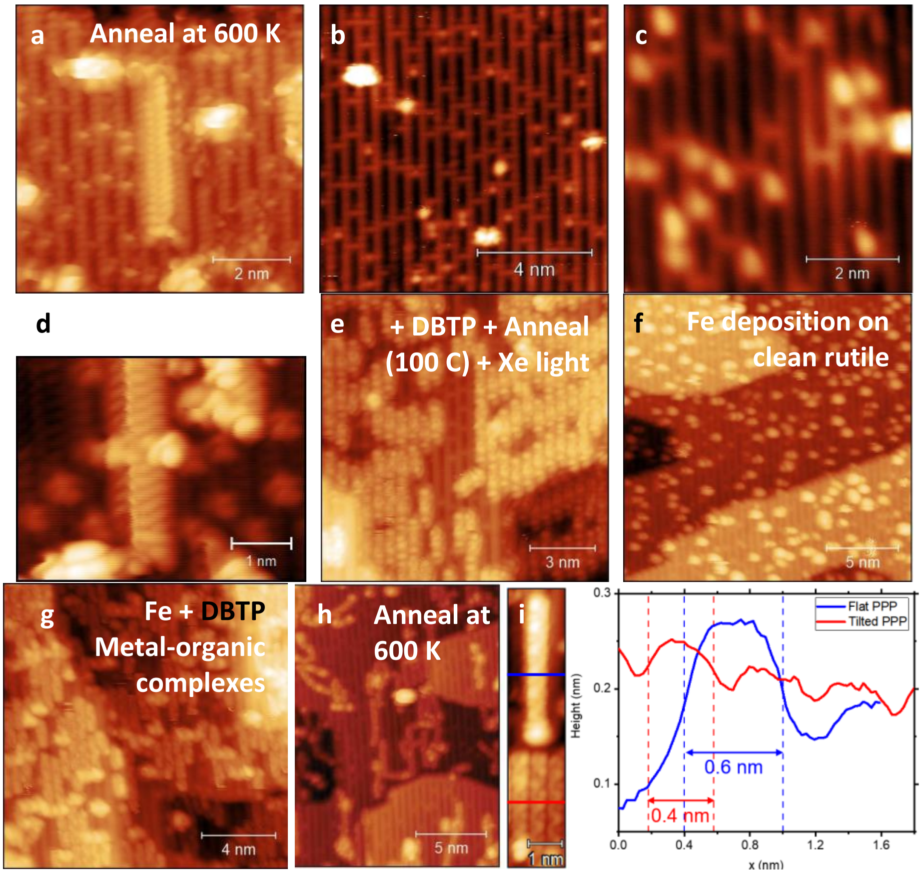

Fig. S4. An STM image of a 2×1 defect on rutile TiO_2 after annealing at 600 K. (a) Z-height = 0.59 nm, V_s = -1 V, I_t = 10 pA. STM images of a clean rutile TiO_2 (110) surface; (b) Z-height = 0.16 nm, V_s = -1 V, I_t = 10 pA. (c) Z-height = 0.12 nm, V_s = -1 V, I_t = 10 pA. An STM image of a 3AGNR on a clean rutile TiO_2 (110) surface after annealing at 600 K; (d) Z-height = 0.39 nm, V_s = -0.5 V, I_t = 10 pA. (e) An STM image of DBTP molecules on a clean rutile TiO_2 (110) surface after annealing at 100 ˚C; Z-height = 0.61 nm, V_s = -1 V, I_t = 10 pA. (f) An STM image of rutile TiO_2 (110) after Fe atoms deposition on this surface; Z-height = 0.89 nm, V_s = -1 V, I_t = 10 pA. (g) An STM image of 3AGNRs on rutile TiO_2 (110) after Fe atoms and DBTP molecules deposition on this surface (sample temperature $\leq$ 0 ˚C) and irradiation by a Xe lamp (filter: 240-395 nm); Z-height = 0.80 nm, V_s = -1 V, I_t = 10 pA. (h) An STM image of PPP wires on a clean rutile TiO_2 (110) surface after annealing a DBTP multilayer at 600 K, in the absence of Fe ad-atoms; Z-height = 0.94 nm, V_s = -1 V, I_t = 10 pA. (i) STM images and the corresponding height profiles of PPP wires on the rutile TiO_2(110) surface after annealing at 500 K (z-height = 0.31 nm). The wider, brighter feature (width $\approx$ 0.6 nm) corresponds to a flat PPP wire, while the thinner, darker features (width $\approx$ 0.4 nm) correspond to tilted PPP wires. STM acquisition temperature: 77 K.

In Fig. S5, annealing DBTP molecules on TiO_2 surfaces leads to the breaking of C-halogen bonds, which are replaced by C-C coupling with lower binding energies. Furthermore, the presence of oxygen vacancies leads to turning Ti^{+4} cations into Ti^{+3} cations, which can be detected by the related shoulder in XPS spectra [6].

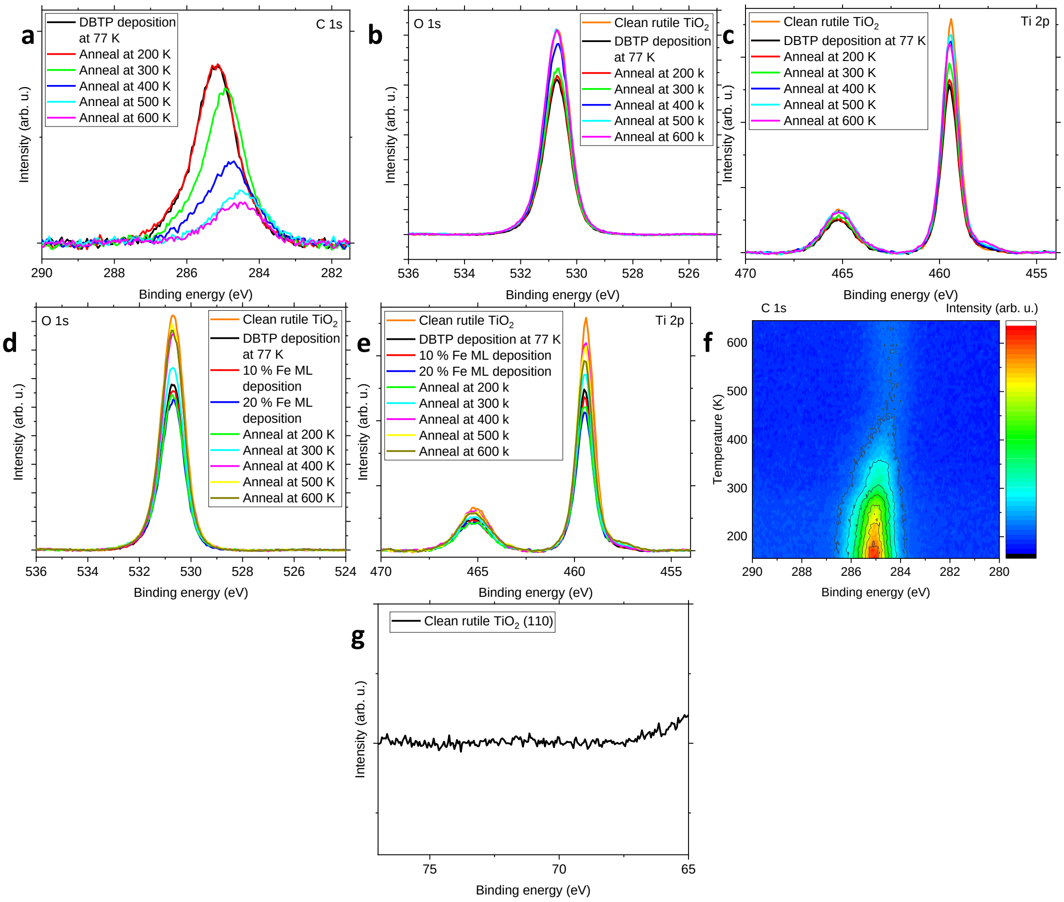

Fig. S5. (a) Br 3d, (b) O 1s, and (c) Ti 2p narrow region XP spectra of a rutile TiO_2 (110) surface after deposition of a DBTP monolayer and annealing the monolayer at different temperatures. (d) O 1s and (d) Ti 2p narrow region XP-spectra of a rutile TiO_2 (110) surface after deposition of a DBTP monolayer and sub-monolayer coverage of Fe atoms (coverages of 10% and 20% ML) and annealing at different temperatures. (f) Temperature-programmed TP-XPS contour of the zoomed-in C 1s core level region after deposition of DBTP molecules on the surface without Fe atoms. (g) Br 3d narrow region XP spectra of a rutile TiO_2 (110) surface after cleaning. XPS acquisition temperature: 77 K.

REFERENCES

(1) Bennett, R. A.; Mulley, J.; Newton, M.; Surman, M. Spectroscopy of ultrathin epitaxial rutile TiO2 (110) films grown on W (100). *J. Chem. Phys.* **2007**, *127* (8).

(2) Fukada, K.; Matsumoto, M.; Takeyasu, K.; Ogura, S.; Fukutani, K. Effects of hydrogen on the electronic state and electric conductivity of the rutile TiO2 (110) surface. *J. Phys. Soc. Jpn.* **2015**, *84* (6), 064716.

(3) Xiong, G.; Shao, R.; Droubay, T. C.; Joly, A. G.; Beck, K. M.; Chambers, S. A.; Hess, W. P. Photoemission electron microscopy of TiO2 anatase films embedded with rutile nanocrystals. *Adv. Funct. Mater.* **2007**, *17* (13), 2133-2138.

(4) Mansfeldova, V.; Zlamalova, M.; Tarabkova, H.; Janda, P.; Vorokhta, M.; Piliai, L.; Kavan, L. Work function of TiO2 (anatase, rutile, and brookite) single crystals: effects of the environment. *J. Phys. Chem. C* **2021**, *125* (3), 1902-1912.

(5) Maheu, C.; Cardenas, L.; Puzenat, E.; Afanasiev, P.; Geantet, C. UPS and UV spectroscopies combined to position the energy levels of TiO 2 anatase and rutile nanopowders. *Phys. Chem. Chem. Phys.* **2018**, *20* (40), 25629-25637.

(6) Scheiber, P.; Fidler, M.; Dulub, O.; Schmid, M.; Diebold, U.; Hou, W.; Aschauer, U.; Selloni, A. (Sub) Surface mobility of oxygen vacancies at the TiO 2 anatase (101) surface. *Phys. Rev. Lett.* **2012**, *109* (13), 136103.